

Performance Analysis of Full-Duplex Relay Networks with Residual Self-Interference and Crosstalk

Guoling Liu, Wenjiang Feng, Bowei Zhang, Tengda Ying and Luran Lü

College of Communication Engineering, Chongqing University

Chongqing, 400044 - P. R. China

[e-mail: {liuguoling, fengwj, 20101213140, 20141201004, 20151202016t}@cqu.edu.cn]

*Corresponding author: Guoling Liu

*Received January 22, 2016; revised July 8, 2016; revised August 12, 2016; accepted August 29, 2016;
published October 31, 2016*

Abstract

This paper investigates the error performance of the amplify-and-forward (AF) relaying systems in the context of full-duplex (FD) communication. In addition to the inherent self-interference (SI) due to simultaneous transmission and reception, coexistent FD terminals may cause crosstalk. In this paper, we utilize the information exchange via the crosstalk channel to construct a particular distributed space-time code (DSTC). The residual SI is also considered. Closed-form pairwise error probability (PEP) is first derived. Then we obtain the upper bound of PEP in high transmit power region to provide more insights of diversity and coding gain. The proposed DSTC scheme can attain full cooperative diversity if the variance of SI is not a function of the transmit power. The coding gain can be improved by lengthening the frame and proper power control. Feasibility and efficiency of the proposed DSTC are verified in numerical simulations.

Keywords: Full-duplex communication, residual self-interference, distributed space-time coding, spatial diversity, cooperative communication

This work is funded by the Chongqing University Graduate Student Research Innovation Project (No. CYB14042).

1. Introduction

Cooperative communication enables multiple single-antenna terminals to create a “virtual” physical array in order to obtain spatial diversity [1, 2]. However, many existing works are based on half-duplex (HD) operation. HD operation requires orthogonal channels (time slots, frequency bands, etc.) to forward the source data, resulting in the loss of spectral efficiency [3]. Many schemes have been proposed to overcome this problem, such as successive relaying [4], frame-level virtual FD relaying [5] and buffer-aided relaying [6]. All of these schemes are based on elaborated designed transmission protocols and more rigorous constraint and have not broken through the fundamental limitation of half-duplexing. In-band full-duplex (IBFD) communication provides the ability of simultaneous transmission and reception in the same frequency band, which gives relay systems the potential to improve spectral efficiency while retaining spatial diversity. An obvious drawback of FD operation is the self-interference (SI) introduced by the leakage of signal and energy from the output to the input of the same terminal. In recent years, a number of studies on self-interference cancellation (SIC) [7-10] have made the FD operation more feasible in practice. SIC aims to reduce the SI to an acceptable level that will not severely affect the detection of the intended signal.

1.1 Related Literature

Earlier researches [11-13] have not taken SI into account. However, the experimental results have pointed out that the SI might not be completely mitigated even with advanced SIC methods. Hence, recent works consider the effect of residual SI on a variety of performance metrics. The authors in [14], [15] study the channel capacity of FD relay networks and stated that FD relaying outperforms its HD counterpart. In [16], it is shown that the unidirectional FD relaying is superior to the two-way HD relaying with physical-layer network coding. Kim et al [17] investigate the optimal power allocation problem in the context of cognitive radio. Rodríguez et al in [18] analysis the non-orthogonal FD amplify-and-forward (AF) relaying in terms of pairwise error probability (PEP). They conclude that even with the presence of residual SI, the FD relaying system can achieve full diversity. In the scenarios where the self-interference might worsen the quality of service, the system tends to operate in the traditional duplex modes. Feng et al. address the duplex mode selection problem in [19] and [20] along with the channel allocation and power control. In common sense, the system benefits more from weaker SI. However, the authors in [21] found that under some conditions, perfect SI cancellation may result in an unstable queue for message storage in a random access multiuser network, which brings a fresh point of view of relay-assisted system design.

Besides single relay networks, the multiple relay networks also draw attention. Some works focus on the parallel relaying systems, i.e., no inter-relay channel exists. In [22], Coso et al. investigate the achievable rates of different relaying protocols, namely: AF, DF, compress-and-forward and linear relaying, in the parallel FD relaying network.

Zamani et al. [23] propose a hybrid decode-amplify forward relaying protocol and obtain its maximum throughput and expected-rate. In the scenarios of satellite-to-satellite communication [24], where isolation of relays can be achieved due to absence of multipath propagation and the SI can be effectively suppressed by directive antennas, significant gains can be achieved by FD operation comparing with HD relaying.

From the practical perspective, coexisted FD relay nodes may cause crosstalk due to essence of simultaneous transmission and reception. Yuksel et al. in [25] show that considering inter-relay communication and clustered network, the relay system can provide high spatial diversity. Without taking residual SI into account, the authors in [26] modeled the cooperative transmission with crosstalk as a partial distributed linear convolutional space-time coding (STC), which can achieve full asynchronous diversity with a minimum means square error and decision feedback equalizer (MMSE-DFE) receivers.

1.2 Contributions and Organization of This Paper

Inspired by the aforementioned studies, we investigate the error performance of uncoded full-duplex AF two-relay systems in the presence of residual SI. In the considered system, two FD relays assist the source node to forward information to the destination node, the direct link is assumed to endure heavy shadow and deep fading such that can be ignored. Crosstalk between the relays is considered as information exchange instead of interference to be mitigated. The main contributions of this paper are summarized as follows:

- 1) The closed-form expression of PEP is derived. Also we obtain the upper bound of PEP in the high transmit power region, which is useful to carry out the diversity and coding gain.
- 2) The diversity gain is discussed with the consideration of residual SI. Theoretical and numerical results show that full diversity is achievable if the variance of residual SI is not a function of the transmit power. Otherwise, the diversity gain is degraded. The scale of degradation is related to the quality of SIC.
- 3) The coding gain is also investigated. Higher coding gain can be obtained by increasing the frame length, surpassing more SI and proper power allocation.

The rest of this paper is organized as follows. The system model and transmission protocol are elaborated in Section 2. The closed-form expression and the upper bound of PEP are worked out in Section 3. Section 4 analyzes the error performance in terms of diversity and coding gain. Numerical results are shown and discussed in Section 5. Finally, conclusion is provided in Section 6.

Notations: In this paper, scalars are denoted with regular lower case letters. Vectors and matrices are denoted with bold lower and upper case letters. We denote \mathbf{A}^H and \mathbf{A}^T as the Hermitian transpose and regular transpose of the matrix \mathbf{A} , respectively. $\det(\cdot)$ stands for the determinant operator. And $\mathbf{E}[\cdot]$ is the expectation operator. \mathbf{I}_N represents the $N \times N$ identity matrix. $\mathbf{Cov}[\cdot]$ is the covariance operator.

2. System Model

Consider a cooperative system which consists of four nodes: one HD source node S , two FD relay nodes R_1 and R_2 , and one HD destination node D , as shown in Fig. 1. All nodes are equipped with single antenna. Since the nodes operate in the same frequency band, the two FD relays may cause crosstalk. We denote the channel from S to R_i ($S \rightarrow R_i$) as f_i , from R_i to D ($R_i \rightarrow D$) as g_i and the crosstalk channel from R_i to R_j as h_{ij} , $i, j \in \{1, 2\}$. By the reciprocity of wireless channels, we have $h_{12} = h_{21} = h$. The Rayleigh block fading is considered, which means that the channel gains remain constant during the transmission period. All the channel gains are assumed to be independent and identically distributed (i.i.d.) cyclic symmetric Gaussian random variables (RV) with zero mean and unit variance. We make the following assumption of CSI: the source has no knowledge of CSI; the relays know the second-order statistics of $S \rightarrow R$ and the crosstalk channels; the destination has global CSI.

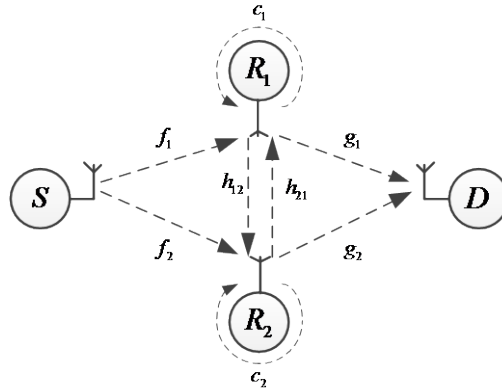


Fig. 1. Two FD relaying system with crosstalk and residual SI

2.1 Transmission Protocol

The source data is transmitted in frame, $\mathbf{s} = [s(1), s(2), \dots, s(T)]^T$. The frame length T is an even number ($T \geq 2$). The transmit signal \mathbf{s} has an expected power equal to one, i.e., $\mathbf{E}[\mathbf{s}^H \mathbf{s}] = 1$. In the t -th time slot, S broadcasts $s(t)$ to the relays. Meanwhile, the relays receive the crosstalk from each other. The received signal at R_i can be written as

$$r_i(t) = \sqrt{P_s T} f_i s(t) + h_{ji} x_j(t) + c_i(t) + n_i(t), \quad i, j \in \{1, 2\}, i \neq j \quad (1)$$

where $c_i(t)$ is the residual SI after SIC, and $n_i(t)$ is the additive white Gaussian noise (AWGN) with zero mean and unit variance. P_s is the transmit power at the source.

$x_i(t)$ is the transmit signal from R_i . The relays amplify and forward the signal which is received in the previous time slot, i.e.,

$$x_i(t) = br_i(t-1), \quad 2 \leq t \leq T \quad (2)$$

where b is the amplification coefficient which will be discussed later. Substituting (2) into (1) we get

$$r_i(t) = \sqrt{P_s T} f_i s(t) + bh_{ji} r_j(t-1) + v_i(t), \quad i, j \in \{1, 2\}, i \neq j \quad (3)$$

where $v_i(t) = c_i(t) + n_i(t)$. Recursively substituting into (3), it can be rewritten as

$$r_i(t) = \sum_{l=1}^t (bh)^{t-l} \left[\sqrt{P_s T} f_k s(l) + v_k(l) \right] \quad (4)$$

where $k=i$ when $(t-l)$ is even, otherwise $k=j$, $i, j \in \{1, 2\}, i \neq j$. Grouping $r_i(t)$ into a vector, the received signal at R_i in T symbol periods can be written as

$$\mathbf{r}_i = \sqrt{P_s T} [\mathbf{B}_1 \mathbf{s} \quad \mathbf{B}_2 \mathbf{s}] \mathbf{f}_{ij} + \mathbf{u}_i \quad (5)$$

where $\mathbf{r}_i = [r_i(1), r_i(1), \dots, r_i(T)]^T$, $\mathbf{f}_{ij} = [f_i \quad f_j]^T$, $\mathbf{u}_i = \mathbf{B}_1 \mathbf{v}_i + \mathbf{B}_2 \mathbf{v}_j$ is the equivalent residual SI plus noise at R_i , $\mathbf{v}_i = [v_i(1), v_i(1), \dots, v_i(T)]^T$ and $\mathbf{v}_j = [v_j(1), v_j(1), \dots, v_j(T)]^T$, $i, j \in \{1, 2\}, i \neq j$, and

$$\mathbf{B}_1 = \begin{cases} b_1^{(m,n)} = (bh)^{(m-n)}, & n \leq m \text{ and } (m-n) \text{ is even} \\ 0, & \text{otherwise} \end{cases}, \quad m, n \in \{1, 2, \dots, T\}$$

$$\mathbf{B}_2 = \begin{cases} b_2^{(m,n)} = (bh)^{(m-n)}, & n \leq m \text{ and } (m-n) \text{ is odd} \\ 0, & \text{otherwise} \end{cases}$$

where $b_1^{(m,n)}$ and $b_2^{(m,n)}$ are the element at the m -th row and n -th column of \mathbf{B}_1 and \mathbf{B}_2 , respectively.

The received signal at D can be written as

$$\begin{aligned} \mathbf{y} &= b[g_1 \mathbf{r}_1 + g_2 \mathbf{r}_2] + \mathbf{n}_d \\ &= \sqrt{P_s T} b [\mathbf{B}_1 \mathbf{s} \quad \mathbf{B}_2 \mathbf{s}] \mathbf{G} \mathbf{f} + b[\mathbf{u}_1 \quad \mathbf{u}_2] \mathbf{g} + \mathbf{n}_d \\ &= \sqrt{P_s T} b \mathbf{M} \mathbf{G} \mathbf{f} + \mathbf{w} \end{aligned} \quad (6)$$

where $\mathbf{M} = [\mathbf{B}_1 \mathbf{s} \quad \mathbf{B}_2 \mathbf{s}]$. $\mathbf{n}_d = [n_d(1), n_d(2), \dots, n_d(T)]^T$ is the AWGN at D , $\mathbf{w} = b[\mathbf{u}_1 \quad \mathbf{u}_2] \mathbf{g} + \mathbf{n}_d$ is the equivalent residual SI plus noise at D , $\mathbf{f} = [f_1 \quad f_2]^T$, $\mathbf{g} = [g_1 \quad g_2]^T$, $\mathbf{G} = \begin{bmatrix} g_1 & g_2 \\ g_2 & g_1 \end{bmatrix}$.

It can be observed from (6) that the uncoded source data \mathbf{s} is transformed into the space-time coded signal \mathbf{M} . The coding matrices \mathbf{B}_1 and \mathbf{B}_2 are not priorly designed and distributed, but involuntarily constructed during the information exchange through the crosstalk channel [26]. We refer to this particular distributed space-time coding (DSTC) scheme as the crosstalk self-coding (CSC). The formation of CSC is built on two preconditions: 1) the bidirectional crosstalk channel between the FD relays; and 2) the non-regenerative (AF) protocol. When operating in HD mode, the relays cannot exchange information simultaneously. Similarly, if the decode-and-forward protocol is employed, the transmit signal from R_i will be treated as interference at R_j , which leads to the failure of information exchange.

It should be noted that we consider the frame length of $T \geq 2$. When $T = 1$, the considered system would regress to a HD relaying system, in which the CSC matrices cannot be constructed. The proposed transmission protocol provides no profit for such a system.

2.2 Statistical Model of Residual Self-Interference

To the best of the authors' knowledge, the accurate relationship between the transmit signal and the residual SI is still unknown in practice. In this paper, we follow the previous works [19, 27] and model the residual SI as an additive Gaussian RV,

$$\mathbf{c}_i(t) \sim CN(\mathbf{0}, \beta P_r^\lambda \mathbf{I}_T) \quad (7)$$

where P_r is the transmit power at each relay, and the values of β ($\beta > 0$) and λ ($0 \leq \lambda \leq 1$) represent the quality of SIC. Smaller β and λ reflect a better SIC performance. In addition, we assume that the residual SI is independent of the signal and noise.

2.3 Amplifying Coefficient

For simplicity, we use the fixed-gain amplification [28]. Since the relays have the same average reception and transmission power, their amplification coefficients can be identical. Note that the consumed power at S and D is P_s and P_r , respectively, the amplifying coefficient can be calculated as

$$b = \sqrt{\frac{\mathbf{E}[\mathbf{x}^H \mathbf{x}]}{\mathbf{E}[\mathbf{r}^H \mathbf{r}]}} = \sqrt{\frac{P_r}{P_s + P_r + \beta P_r^\lambda + 1}} \quad (8)$$

In the proposed system, a special case should be considered: At time slot $t = 1$, the relays keep silence, therefore no SI exists. At time slot $t = 2$, the power of received signal at each relay is higher than that in the last time slot because of the appearance of SI. By parity of reasoning, the average transmit power consumed by the relays at each time slot will increase with t . As shown in (7), the variance of residual SI is related to P_r . Hence, the accumulation of P_r will worsen the average signal to interference plus noise

ratio (SINR) at D . We propose a simple solution to simultaneously fix the amplifying coefficient and transmit power: At time slot $t=1$, each relay transmits a deterministic symbol s_0 with the power of P_r . Then, the power of received signal at time slot $t=2$ equals to that at time slot $t=1$, and so on. When T is large, the loss of power efficiency at the relays can be neglected. Since D has global CSI, the corresponding terms of s_0 can be directly removed from the received signal and will not affect the error performance. In the rest of this paper, the terms of s_0 will be omitted for clarity.

3. Pairwise Error Probability

3.1 Maximum Likelihood Detection

Given that D has global CSI, \mathbf{w} is a Gaussian RV with zero mean and the variance of $\mathbf{R}_{\mathbf{w}\mathbf{w}} = \mathbf{E}[\mathbf{w}\mathbf{w}^H]$. Assume that a message \mathbf{s}_p is transmitted from S , then the conditional received signal $\mathbf{y}|\mathbf{s}_p$ is also a Gaussian random vector with the mean of $\sqrt{P_s T} b \mathbf{M}_p \mathbf{G} \mathbf{f}$ and the variance of $\mathbf{R}_{\mathbf{w}\mathbf{w}}$. The probability density function of $\mathbf{y}|\mathbf{s}_p$ can be written as

$$P(\mathbf{y}|\mathbf{s}_p) = \frac{\exp\left(-\left(\mathbf{y} - \sqrt{P_s T} b \mathbf{M}_p \mathbf{G} \mathbf{f}\right)^H \mathbf{R}_{\mathbf{w}\mathbf{w}}^{-1} \left(\mathbf{y} - \sqrt{P_s T} b \mathbf{M}_p \mathbf{G} \mathbf{f}\right)\right)}{\pi^T \det(\mathbf{R}_{\mathbf{w}\mathbf{w}})} \quad (9)$$

where $\mathbf{M}_p = [\mathbf{B}_1 \mathbf{s}_p \quad \mathbf{B}_2 \mathbf{s}_p]$. Thus, the ML detection can be straightforward given as

$$\arg \max_{\mathbf{s}_p} P(\mathbf{y}|\mathbf{s}_p) = \arg \min_{\mathbf{s}_p} \left\| \mathbf{y} - \sqrt{P_s T} b \mathbf{M}_p \mathbf{G} \mathbf{f} \right\|^2 \quad (10)$$

3.2 Pairwise Error Probability

Based on the ML detector in (10), the PEP of mistaking \mathbf{s}_p by \mathbf{s}_q , under certain channel realization, can be written as

$$P(\mathbf{s}_p \rightarrow \mathbf{s}_q | f_i, g_i) = P\left(\left\| \mathbf{y} - \sqrt{P_s T} b \mathbf{M}_p \mathbf{G} \mathbf{f} \right\|^2 > \left\| \mathbf{y} - \sqrt{P_s T} b \mathbf{M}_q \mathbf{G} \mathbf{f} \right\|^2 | f_i, g_i\right) \quad (11)$$

where $\mathbf{M}_q = [\mathbf{B}_1 \mathbf{s}_q \quad \mathbf{B}_2 \mathbf{s}_q]$. Equation (11) provides the exact PEP of the considered system. However, the calculation of (11) is very hard and gives little insights. The rest of this section will focus on the upper bound of PEP which is more analyzable and tractable.

As a first step, we upper bound the PEP in (11) by the Chernoff bound. The main result is presented in the following theorem.

Theorem 1: With the ML detector in (10), the PEP of the considered system has the Chernoff bound of

$$P(\mathbf{s}_p \rightarrow \mathbf{s}_q | f_i, g_i) \leq \mathbf{E}_{f_i, g_i} \left[\exp \left(- \frac{P_s T b^2 \mathbf{f}^H \mathbf{G}^H \tilde{\mathbf{M}} \mathbf{G} \mathbf{f}}{4 \left[b^2 (|g_1|^2 + |g_1|^2) (1 + \beta P_r^\lambda) \sigma_{max}^2 + 1 \right]} \right) \right] \quad (12)$$

where $\tilde{\mathbf{M}} = (\mathbf{M}_p - \mathbf{M}_q)^H (\mathbf{M}_p - \mathbf{M}_q)$.

Proof: As in [29] and [30], the PEP in (9) has the Chernoff bound of

$$P(\mathbf{s}_p \rightarrow \mathbf{s}_q | f_i, g_i) \leq \mathbf{E}_{f_i, g_i} \left[\exp \left(\lambda \left[\ln P(\mathbf{y} | \mathbf{s}_p) - \ln P(\mathbf{y} | \mathbf{s}_q) \right] \right) \right] \quad (13)$$

By (9), the exponent on the right-hand side of (13) can be written as

$$\begin{aligned} \ln P(\mathbf{y} | \mathbf{s}_p) - \ln P(\mathbf{y} | \mathbf{s}_q) = & -P_s T b^2 \mathbf{f}^H \mathbf{G}^H (\mathbf{M}_p - \mathbf{M}_q)^H \mathbf{R}_{\mathbf{w}\mathbf{w}}^{-1} (\mathbf{M}_p - \mathbf{M}_q) \mathbf{G} \mathbf{f} \\ & - \sqrt{P_s T} b \mathbf{f}^H \mathbf{G}^H (\mathbf{M}_p - \mathbf{M}_q)^H \mathbf{R}_{\mathbf{w}\mathbf{w}}^{-1} \mathbf{w} - \sqrt{P_s T} b \mathbf{w} \mathbf{R}_{\mathbf{w}\mathbf{w}}^{-1} (\mathbf{M}_p - \mathbf{M}_q) \mathbf{G} \mathbf{f} \end{aligned} \quad (14)$$

Substituting (14) into (13) yields the following equation after some simplification

$$P(\mathbf{s}_p \rightarrow \mathbf{s}_q | f_i, g_i) \leq \mathbf{E}_{f_i, g_i} \left[\exp \left(-\lambda(1-\lambda) P_s T b^2 \mathbf{f}^H \mathbf{G}^H (\mathbf{M}_p - \mathbf{M}_q)^H \mathbf{R}_{\mathbf{w}\mathbf{w}}^{-1} (\mathbf{M}_p - \mathbf{M}_q) \mathbf{G} \mathbf{f} \right) \right] \quad (15)$$

Let $\lambda = \frac{1}{2}$, we have $-\lambda(1-\lambda) = -1/4$, which minimizes the exponent at the right-hand side of (15). Due to the accumulation of residual SI and noise, \mathbf{w} is non-white and non-stationary, which complicates the calculation of $\mathbf{R}_{\mathbf{w}\mathbf{w}}^{-1}$. In this paper, we use the approximation of the worst-case stationary residual SI and noise to upper bound (15), i.e., we use $\mathbf{w}' = [w(T), w(T), \dots, w(T)]^T$ to substitute \mathbf{w} in (6), where $w(T)$ is the T -th entry of \mathbf{w} . Therefore, we have

$$\mathbf{R}_{\mathbf{w}'\mathbf{w}'}^{-1} = \frac{1}{b^2 (|g_1|^2 + |g_1|^2) (1 + \beta P_r^\lambda) \sigma_{max}^2 + 1} \mathbf{I}_T \quad (16)$$

where $\sigma_{max}^2 = \sum_{i=0}^{T-1} (bh)^{2i}$. By now, (15) can be upper bounded by (12) and the proof ends here.

Averaging (12) over \mathbf{f} , we have

$$\begin{aligned} P(\mathbf{s}_p \rightarrow \mathbf{s}_q | g_i) & \leq \mathbf{E}_{g_i} \left[\int_{\mathbf{f} \in \mathbb{C}^{2d}} \exp \left(- \frac{P_s T b^2 \mathbf{f}^H \mathbf{G}^H \tilde{\mathbf{M}} \mathbf{G} \mathbf{f}}{4 \left[b^2 (|g_1|^2 + |g_1|^2) (1 + \beta P_r^\lambda) \sigma_{max}^2 + 1 \right]} \right) \frac{\exp(-\mathbf{f}^H \mathbf{f})}{\pi^2} d\mathbf{f} \right] \\ & = \mathbf{E}_{g_i} \left[\det^{-1} \left(\mathbf{I}_2 + \frac{P_s T b^2 \tilde{\mathbf{M}} \tilde{\mathbf{G}}}{4 \left[b^2 (|g_1|^2 + |g_1|^2) (1 + \beta P_r^\lambda) \sigma_{max}^2 + 1 \right]} \right) \right] \end{aligned} \quad (17)$$

where $\tilde{\mathbf{G}} = \mathbf{G}^H \mathbf{G}$. In the last step of (17), we use the fact that $E[e^{-\mathbf{u}^H \mathbf{K} \mathbf{u}}] = \det^{-1}(\mathbf{I} + \mathbf{R} \mathbf{K})$, for a given Gaussian random vector \mathbf{u} subject to $CN(0, \mathbf{R})$ and a Hermitian matrix \mathbf{K} . Also we use the fact that $\det(\mathbf{I} + \mathbf{A} \mathbf{B}) = \det(\mathbf{I} + \mathbf{B} \mathbf{A})$ where \mathbf{B} and \mathbf{A} have proper dimensions.

Substituting (8) into (17), we have

$$P(\mathbf{s}_p \rightarrow \mathbf{s}_q | g_i) \leq \mathbf{E}_{g_i} \left[\det^{-1}(\mathbf{I}_2 + \rho \tilde{\mathbf{M}} \tilde{\mathbf{G}}) \right] \quad (18)$$

where $\rho = \frac{P_s P_r T}{4 \left[P_r (\beta P_r^\lambda + 1) (|g_1|^2 + |g_2|^2) \sigma_{\max}^2 + P_s + \beta P_r^\lambda + 1 \right]}$. In the high transmit power regime, i.e., $P_s \rightarrow \infty$ and $P_r \rightarrow \infty$, $\rho \approx \frac{P_s P_r T}{4 \beta \sigma_{\max}^2 P_r^{1+\lambda} (|g_1|^2 + |g_2|^2)}$. Since $\tilde{\mathbf{G}}$ is

Hermitian, we can perform the eigendecomposition on $\tilde{\mathbf{G}}$,

$$\tilde{\mathbf{G}} = \mathbf{Q} \mathbf{\Gamma} \mathbf{Q}^H = \begin{bmatrix} 1/\sqrt{2} & 1/\sqrt{2} \\ 1/\sqrt{2} & -1/\sqrt{2} \end{bmatrix} \begin{bmatrix} |g_1 + g_2|^2 & 0 \\ 0 & |g_1 - g_2|^2 \end{bmatrix} \begin{bmatrix} 1/\sqrt{2} & 1/\sqrt{2} \\ 1/\sqrt{2} & -1/\sqrt{2} \end{bmatrix} \quad (19)$$

where \mathbf{Q} is a unitary matrix, and $\mathbf{\Gamma}$ is a diagonal matrix that contains the eigenvalues of $\tilde{\mathbf{G}}$. Combining \mathbf{Q} and \mathbf{Q}^H with $\tilde{\mathbf{M}}$, the upper bound of PEP in (16) can be rewritten as

$$P(\mathbf{s}_p \rightarrow \mathbf{s}_q | g_i) \leq \mathbf{E}_{g_i} \left[\det^{-1}(\mathbf{I}_2 + \rho \tilde{\mathbf{M}} \mathbf{\Gamma}) \right] \quad (20)$$

where $\tilde{\mathbf{M}} = \mathbf{Q} \tilde{\mathbf{M}} \mathbf{Q}^H$. Denote $z_1 = g_1 + g_2$, $z_2 = g_1 - g_2$, and $\tilde{\mathbf{M}} = \begin{bmatrix} \gamma_{11} & \gamma_{12} \\ \gamma_{21} & \gamma_{22} \end{bmatrix}$. The determinant on the right-hand side of (20) can be trivially rewritten as

$$\begin{aligned} \det(\mathbf{I}_2 + \rho \tilde{\mathbf{M}} \mathbf{\Gamma}) &= \det \left(\begin{bmatrix} 1 & 0 \\ 0 & 1 \end{bmatrix} + \rho \begin{bmatrix} \gamma_{11} & \gamma_{12} \\ \gamma_{21} & \gamma_{22} \end{bmatrix} \begin{bmatrix} |z_1|^2 & 0 \\ 0 & |z_2|^2 \end{bmatrix} \right) \\ &= \rho^2 \det \left(\begin{bmatrix} |z_1|^2 \gamma_{11} + 1 & |z_2|^2 \gamma_{12} \\ |z_1|^2 \gamma_{21} & |z_2|^2 \gamma_{22} + 1 \end{bmatrix} \right) \\ &= \rho^2 \left[(|z_1|^2 \gamma_{11} + 1) (|z_2|^2 \gamma_{22} + 1) - |z_1|^2 |z_2|^2 \gamma_{12} \gamma_{21} \right] \\ &= \rho^2 \left(\det(\tilde{\mathbf{M}}) |z_1|^2 |z_2|^2 + |z_1|^2 \gamma_{11} + |z_2|^2 \gamma_{22} + 1 \right) \end{aligned} \quad (21)$$

Recall that $\tilde{\mathbf{M}}$ is the Gram matrix of two linear independent vectors $\mathbf{B}_1 \hat{\mathbf{s}}$ and $\mathbf{B}_2 \hat{\mathbf{s}}$,

where $\hat{\mathbf{s}} = \mathbf{s}_p - \mathbf{s}_q$. So we have $\gamma_{11} \geq 0$ and $\gamma_{22} \geq 0$. The determinant on the right-hand side of (21) can be lower bounded as

$$\det(\mathbf{I}_2 + \rho \tilde{\mathbf{M}} \Gamma) \geq \rho^2 \det(\tilde{\mathbf{M}}) |z_1|^2 |z_2|^2 \quad (22)$$

By (20), the upper bound of PEP in (20) can be updated as

$$P(\mathbf{s}_p \rightarrow \mathbf{s}_q \mid |z_i|^2) \leq \mathbf{E}_{|z_i|^2} \left[\frac{\det^{-1}(\tilde{\mathbf{M}})}{\rho^2 |z_1|^2 |z_2|^2} \right] \quad (23)$$

3.3 Discussion on Correlation between $R_i \rightarrow D$ links

The diagonal elements of Γ is the equivalent power gains of the $R_i \rightarrow D$ links. Due to the information exchange between the relays, the original channel coefficients g_1 and g_2 are now transformed to the compounded channel coefficients $g_1 + g_2$ and $g_1 - g_2$. From the perspective of conventional multiple-input-multiple-output or space-time code analysis, the correlation among different channel coefficients directly affects the achievable diversity. If the channels are statistically independent, the system has potential to achieve full diversity; otherwise the diversity order is degraded. To that end, we need to explore the relationship between the two compounded channel coefficients. By introducing the following two useful lemmas [31], we can prove that $g_1 + g_2$ and $g_1 - g_2$ are statistically independent.

Lemma 1: Joint Gaussian RVs arise from nonsingular linear transformations on independent normal RVs.

Lemma 2: If X_1, X_2, \dots, X_n are jointly Gaussian and uncorrelated, then the X_i are independent.

Given that z_1 and z_2 are Gaussian distributed, we have

$$\begin{bmatrix} z_1 \\ z_2 \end{bmatrix} = \begin{bmatrix} 1 & 1 \\ 1 & -1 \end{bmatrix} \begin{bmatrix} g_1 \\ g_2 \end{bmatrix} \quad (24)$$

The above equation points out that z_1 and z_2 are joint Gaussian according to Lemma 1. The covariance of z_1 and z_2 can be calculated as

$$\begin{aligned} \mathbf{Cov}[z_1, z_2] &= \mathbf{E}[z_1 z_2^*] - \mathbf{E}[z_1] \mathbf{E}[z_2^*] \\ &= \mathbf{E}[|g_1|^2] - \mathbf{E}[|g_2|^2] \\ &= 0 \end{aligned} \quad (25)$$

which suggests that z_1 and z_2 are also uncorrelated. So we can conclude that z_1 and z_2 are statistically independent by Lemma 2, and the considered system has the potential to achieve full diversity.

4. Derivation of Diversity and Coding Gain

In this section, we will derive the diversity and coding gain of the considered system based on the derived upper bound of PEP, and provide some remarks on the theoretical results.

Note that z_i , $i \in \{1, 2\}$, is a linear combination of two independent Gaussian RVs, so $|z_i|^2$ has the exponential distribution of

$$P_{|z_i|^2}(x) = e^{-x} \quad (26)$$

Assume that the total consumed power of the considered system is P and $P_s = \alpha P$, we have $P_r = \frac{1-\alpha}{2}P$, $0 < \alpha < 1$. The upper bound in (23) can be calculated as

$$\begin{aligned} P(\mathbf{s}_p \rightarrow \mathbf{s}_q | |z_i|^2) &\leq \lim_{x \rightarrow 0} \int_x^\infty \int_x^\infty \frac{\det^{-1}(\tilde{\mathbf{M}})}{\rho^2 |z_1|^2 |z_2|^2} \exp[-(|z_1|^2 + |z_2|^2)] d|z_1|^2 d|z_2|^2 \\ &= \lim_{x \rightarrow 0} \left(\frac{4\beta\sigma_{max}^2 P_r^{1+\lambda}}{P_s P_r T} \right)^2 \det^{-1}(\tilde{\mathbf{M}}) [2e^{-2x} + e^{-x}(1+x)(-2\text{Ei}(-x) + \ln x)] \quad (27) \\ &\approx \left[\frac{2^{2-\lambda} (1-\alpha)^\lambda \beta\sigma_{max}^2 P^{\lambda-1}}{\alpha T} \right]^2 \det^{-1}(\tilde{\mathbf{M}}) [-2\text{Ei}(-x) + \ln x] \end{aligned}$$

The diversity and coding gain can be worked out through (27), the main results are summarized in the following theorem.

Theorem 2: The PEP of the considered system can be upper bounded by

$$P(\mathbf{s}_p \rightarrow \mathbf{s}_q) \leq \left[\frac{2^{2-\lambda} (1-\alpha)^\lambda \beta\sigma_{max}^2}{\alpha T} \right]^2 \det^{-1}(\tilde{\mathbf{M}}) P^{-2(1-\lambda)} \ln P \quad (28)$$

Proof: Set $x = 1/P$ in (28). When $P \gg 1$, we have $1/P \rightarrow 0$ which corresponds to the assumption of $x \rightarrow 0$. Also, we have $-\text{Ei}(-x) = -\text{Ei}(-1/P) = \ln P + O(1)$. By omitting the lower-order terms of P , we obtain the expression in (28).

Remarks on Theorem 2:

1) The proposed CSC scheme achieves the diversity of $2(1-\lambda) - \ln \ln P / \ln P$, which is jointly determined by the transmit power P and the quality of SI suppression λ . When $\lambda = 0$, the system achieves full diversity. The considered system needs efficient SIC to guarantee an acceptable diversity order, because the diversity order decays linearly with λ . In Section 2, we use two parameters, λ and β , to characterize the variance of SI. However, the diversity order does not involve β . Therefore, full diversity is achievable in the presence of residual SI if and only if the variance of residual SI is not a function of the transmit power at the relays.

2) The achievability of full diversity is also built on the full rank of $\tilde{\mathbf{M}}$, or essentially $\tilde{\mathbf{M}}$. In the studies of STC, $\tilde{\mathbf{M}}$ is usually referred to as the coding gain distance (CGD) matrix. If $\tilde{\mathbf{M}}$ drops rank, the diversity order decreases. The detailed expression of $\tilde{\mathbf{M}}$ is

$$\tilde{\mathbf{M}} = \begin{bmatrix} \hat{\mathbf{s}}\mathbf{B}_1^H\mathbf{B}_1\hat{\mathbf{s}} & \hat{\mathbf{s}}\mathbf{B}_1^H\mathbf{B}_2\hat{\mathbf{s}} \\ \hat{\mathbf{s}}\mathbf{B}_2^H\mathbf{B}_1\hat{\mathbf{s}} & \hat{\mathbf{s}}\mathbf{B}_2^H\mathbf{B}_2\hat{\mathbf{s}} \end{bmatrix} \quad (29)$$

From (29) we know that if $\mathbf{B}_1 \neq \mathbf{B}_2$, $\tilde{\mathbf{M}}$ has full rank. When $h \neq 0$, $\mathbf{B}_1 \neq \mathbf{B}_2$ holds according to the definition of \mathbf{B}_1 and \mathbf{B}_2 in (5). When $h=0$, \mathbf{B}_1 becomes an identity matrix, \mathbf{B}_2 becomes a zero matrix, and $\tilde{\mathbf{M}}$ would be rank-one. In Section 2, we assume that h is subject to complex Gaussian distribution with zero mean and unit variance. The probability of $h=0$ is zero. Hence, $\tilde{\mathbf{M}}$ is full rank with probability one.

3) The crosstalk channel coefficient h should be treated as a deterministic and known complex at D . Note that each non-zero elements in \mathbf{B}_2 contains an odd-order moment of h . If we consider h as an RV, \mathbf{B}_2 will vanish since all odd-order moments of a Gaussian RV are zero, and the structure of CSC will be completely destroyed. Therefore, in the calculation of error probability, h should not be averaged over [26].

4) The term $-\ln \ln P / \ln P$ in the diversity order can also be observed in other relay systems, such as the HD DSTC and the FD NAF relaying. The reason is that the fading $R \rightarrow D$ links make the equivalent noise at the destination not Gaussian distributed. Comparing with the FD NAF system whose diversity order is $2 - \ln \ln P / \ln P$, the considered system in this paper has an additional reduction of -2λ . This is because that in the NAF systems, the signal conveyed in the direct link does not suffer from SI. However, in our work, all signals received from the relays are corrupted by residual SI at the relays.

5) Theorem 2 also shows the coding gain, which is

$$\left[\frac{\alpha T}{2^{2-\lambda} (1-\alpha)^\lambda \beta \sigma_{\max}^2} \right]^2 \det(\tilde{\mathbf{M}}) \quad (30)$$

Equation (30) reveals that the coding gain is dominated by the frame length T , the power control factor α , and the quality of SIC β and λ . We do not involve $\det(\tilde{\mathbf{M}})$ and σ_{\max}^2 , because in a given realization of the inter-relay channel, $\det(\tilde{\mathbf{M}})$ and σ_{\max}^2 are determined by T and α . Due to the complicated relationship among the parameters in (30), we cannot precisely delineate the behavior of the coding gain. Alternatively, characters of the coding gain are demonstrated by numerical simulation in the next section.

5. Numerical Results

In this section, we present the numerical simulations of the proposed CSC scheme to verify the theoretical results. The simulations are divided into 2 parts: 1) the comparisons of the CSC scheme with the HD Alamouti STC [32], and existing full-duplex relay-assisted transmission schemes, such as the FD-NAF in [19] and the PDLC-STC in [26]; and 2) the illustration of the proposed CSC scheme with different quality of SIC λ , and frame length T .

All channel gains are realized as i.i.d. complex Gaussian RVs with zero mean and unit variance, and keep constant during the transmission period. And all noises at the relays and the destination are also modeled as AWGN with zero mean and unit variance. The residual SI is realized as AWGN with zero mean, and the variance shown in (7). In all simulations, the transmit power P at the source and relays is normalized by the noise power and presented in decibel. Other involved parameters are listed in the following table.

Table 1. Configuration of the simulations

	Crosstalk Self-Coding (FD)	PDLC-STC (FD)	Non-Orthogonal Relaying (FD)	Alamouti STC (HD)
Number of Bits	10^6	10^6	10^6	10^6
Modulation Scheme	QPSK	QPSK	QPSK	16-QAM
Frame Length	5	5	5	5
Power Control	$P_s = \frac{P}{2}, P_r = \frac{P}{4}$	--	$P_s = P_r = P$	$P_s = \frac{P}{2}, P_r = \frac{P}{4}$
Decoding Algorithm	Sphere Decoding [33]	MMSE-DFE	Sphere Decoding	Sphere Decoding
Power Range	0~40dB	0~40dB	0~40dB	0~40dB

Simulation A: This simulation illustrates the BER performance of the proposed CSC scheme, along with the NAF scheme, PDLC-STC scheme, and the HD Alamouti STC, against the total consumed power P . The configuration of the simulation scenario is shown in Table 1. For all the FD scheme, we set $\lambda = 0.1$. The results are shown in Fig. 2.

Due to the SI-free direct link between the source and the destination, the FD-NAF system with the diversity order of 2 (full diversity) has the best error performance. The CSC scheme with the diversity order of $1 - \lambda = 1.8$ achieves a little higher BER, since the CSC scheme is built on a dual-hop system where all signal is corrupted by SI. On the other hand, thanks to the inherent advantage of ML decoder over the MMSE-DFE decoder, the CSC scheme outperforms the PDLC-STC scheme when $P > 15\text{dB}$. The MMSE-DFE decoder performs symbol-by-symbol decoding and may cause error

propagation, instead the ML decoder makes considerable improvement by jointly decoding all received symbols.

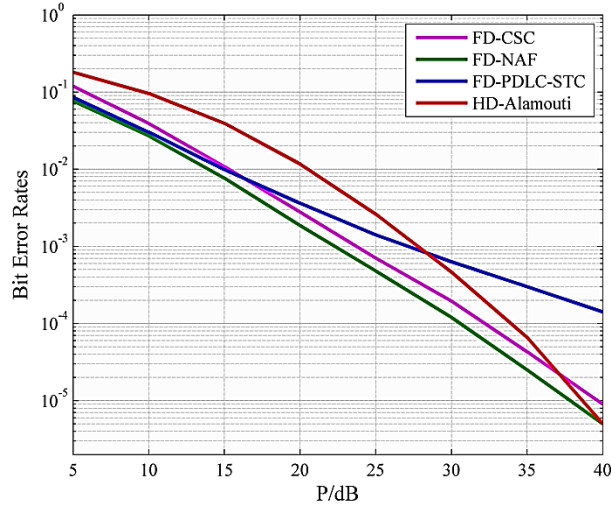


Fig. 2. BER performance of the proposed CSC scheme against the total consumed power P

A counter-intuitive phenomenon occurs in the comparison of the CSC scheme and the HD Alamouti STC. For $P < 37\text{dB}$, the CSC scheme outperforms the HD Alamouti STC; otherwise the Alamouti STC is superior. By common sense, the HD systems do not suffer from SI and should have better error performance than its FD counterparts. This contradiction can be explained in two aspects: 1) The HD Alamouti STC scheme employs higher-order modulation to achieve the same rate as the CSC scheme; 2) The CSC scheme provides coding gain which is absent in the Alamouti STC scheme. These extra improvements compensate the loss of error performance caused by SI. In a word, for a certain rate, the FD system with CSC is more reliable in practical transmit power regime. [16] has the similar conclusion for the FD-NAF systems.

Table 2. Diversity orders under different λ

λ	Diversity Order (Omitting the term of $\ln \ln P / \ln P$)
0.1	1.8
0.2	1.6
0.5	1.0
1.0	0

Simulation B: Fig. 3 shows the BER performance of the proposed CSC scheme under different λ . Other parameters in this simulation are identical to Simulation A. The

theoretical diversity orders under different λ are listed in [Table 2](#).

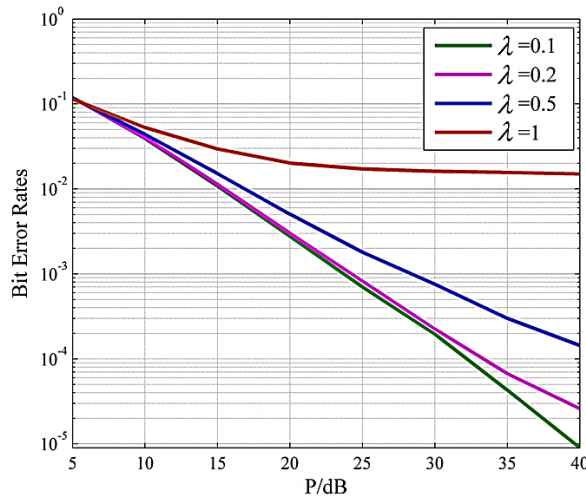


Fig. 3. BER performance of the proposed CSC scheme under different quality of SIC

Clearly, the BER performance is degraded rapidly with the increase of λ , and an error floor can be observed when $\lambda = 1$, which is in agreement of the diversity analysis in Remark 1) on Theorem 2. [Fig. 3](#) reveals that the diversity gain is highly sensitive to λ , which means that a well-designed SIC method significantly helps the considered system to attain lower BER level.

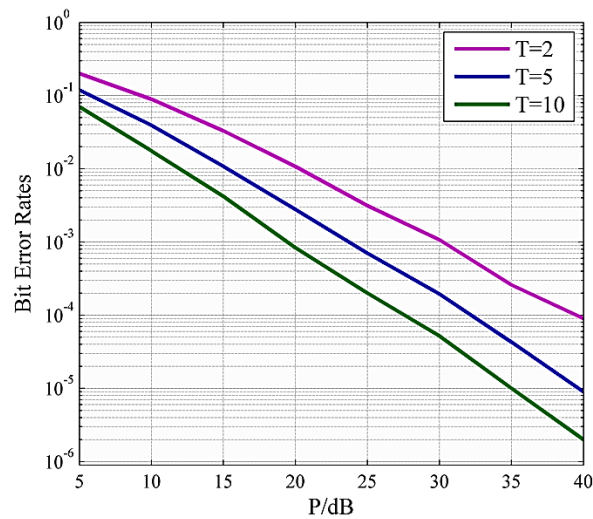


Fig. 4. BER performance of the proposed CSC scheme under different frame length

Simulation C: Effects on BER performance of the frame length T is illustrated in Fig. 4. We can see that at the same transmit power level, the BER decreases with T , which indicates that the lengthening the frame increases the coding gain as proved in Theorem 2. However, it can be observed that increasing T from 2 to 5 provides more BER decrease than increasing T from 5 to 10. The reason is that larger T results more accumulation of SI and noise, i.e., larger σ_{\max}^2 in (30). And a larger σ_{\max}^2 decreases the coding gain in reverse. Generally speaking, increasing T improves the BER, but excessive increase provides less benefits.

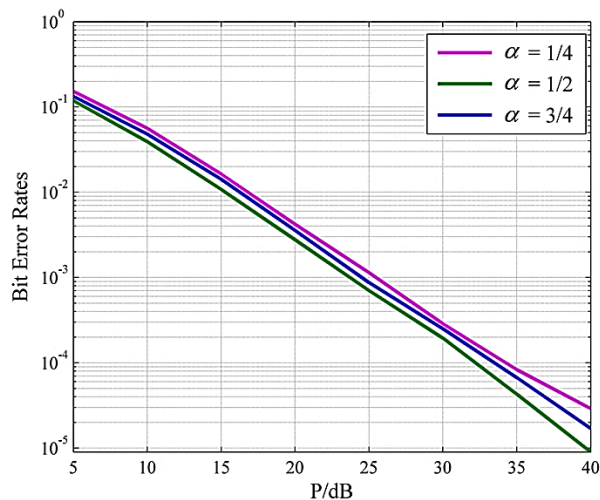


Fig. 5. BER performance of the proposed CSC scheme under different power allocation

Simulation D: The BER performance of CSC is demonstrated in Fig. 5. Comparing with the frame length, the power control scheme makes less contribution to the BER improvement. Fig. 5 shows an interesting result that there is a tradeoff in allocation power between the source and the relays. This can be easily explained as following: When $\alpha = 1/4$, the signals at the destination will be severely interfered due to the higher power at the relays; when $\alpha = 3/4$, the power of intended signal is small at the destination. And setting $\alpha = 1/2$ may reach a rough equilibrium between the SINR at the relays and that at the destination.

6. Conclusion

This paper investigated the error performance of uncoded full-duplex AF two-relay cooperative systems in the presence of residual self-interference. Crosstalk between relays introduced by the FD operation was regarded as self-coding rather than interference and utilized to improve spatial diversity. A closed-form expression of the

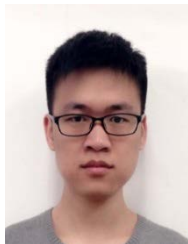
PEP was derived. The upper bound of PEP in high transmit power region was obtained to discuss the diversity and coding gain. It was shown that full cooperative diversity can be achieved when the variance of the residual SI is not a function of the transmit power. Otherwise, the diversity gain decreases linearly with the quality of SIC λ . In addition, the coding gain is principally determined by the frame length, and the power control factor. Generally speaking, λ plays a critical role in error performance of the considered system, and the validity of CSC is built on the ML decoder, efficient SIC, sufficient long frame and proper power control scheme.

References

- [1] J. N. Laneman and G. W. Wornell, "Distributed space-time-coded protocols for exploiting cooperative diversity in wireless networks," *IEEE Transactions on Information Theory*, vol. 49, no. 10, pp. 2415-2425, Oct. 2003. [Article \(CrossRef Link\)](#).
- [2] J. N. Laneman, D. N. C. Tse and G. W. Wornell, "Cooperative diversity in wireless networks: Efficient protocols and outage behavior," *IEEE Transactions on Information Theory*, vol. 50, no. 12, pp. 3062-3080, Dec. 2004. [Article \(CrossRef Link\)](#).
- [3] K. Azarian, H. El Gamal and P. Schniter, "On the achievable diversity-multiplexing tradeoff in half-duplex cooperative channels," *IEEE Transactions on Information Theory*, vol. 51, no. 12, pp. 4152-4172, Dec. 2005. [Article \(CrossRef Link\)](#).
- [4] Y. Fan, C. Wang, J. Thompson and H. V. Poor, "Recovering Multiplexing Loss through Successive Relaying Using Repetition Coding," *IEEE Transactions on Wireless Communications*, vol. 6, no. 12, pp. 4484-4493, December 2007. [Article \(CrossRef Link\)](#).
- [5] L. Zhang and D. Guo, "Virtual Full Duplex Wireless Broadcasting via Compressed Sensing," *IEEE/ACM Transactions on Networking*, vol. 22, no. 5, pp. 1659-1671, Oct. 2014. [Article \(CrossRef Link\)](#).
- [6] N. Nomikos et al., "A Survey on Buffer-Aided Relay Selection," *IEEE Communications Surveys & Tutorials*, vol. 18, no. 2, pp. 1073-1097, Secondquarter 2016. [Article \(CrossRef Link\)](#).
- [7] Y. Y. Kang, B. J. Kwak and J. H. Cho, "An Optimal Full-Duplex AF Relay for Joint Analog and Digital Domain Self-Interference Cancellation," *IEEE Transactions on Communications*, vol. 62, no. 8, pp. 2758-2772, Aug. 2014. [Article \(CrossRef Link\)](#).
- [8] M. Jain et al., "Practical, real-time, full duplex wireless," in *Proc. of ACM Mobicom*, Las Vegas, NV, USA, pp. 301-312, Sep. 2011. [Article \(CrossRef Link\)](#).
- [9] A. Sabharwal, P. Schniter, D. Guo, D. W. Bliss, S. Rangarajan and R. Wichman, "In-Band Full-Duplex Wireless: Challenges and Opportunities," *IEEE Journal on Selected Areas in Communications*, vol. 32, no. 9, pp. 1637-1652, Sept. 2014. [Article \(CrossRef Link\)](#).
- [10] D. Bharadia et al., "Full duplex radios," in *Proc. of ACM SIGCOMM*, New York, NY, USA, pp. 375-386, Aug. 2011. [Article \(CrossRef Link\)](#).
- [11] T. Cover and A. E. Gamal, "Capacity theorems for the relay channel," *IEEE Transactions on Information Theory*, vol. 25, no. 5, pp. 572-584, Sep 1979. [Article \(CrossRef Link\)](#).
- [12] Y. Zou, Y. D. Yao and B. Zheng, "Opportunistic Distributed Space-Time Coding for Decode-and-Forward Cooperation Systems," *IEEE Transactions on Signal Processing*, vol. 60, no. 4, pp. 1766-1781, April 2012. [Article \(CrossRef Link\)](#).

- [13] D. W. K. Ng, E. S. Lo and R. Schober, "Dynamic Resource Allocation in MIMO-OFDMA Systems with Full-Duplex and Hybrid Relaying," *IEEE Transactions on Communications*, vol. 60, no. 5, pp. 1291-1304, May 2012. [Article \(CrossRef Link\)](#).
- [14] Y. Y. Kang and J. H. Cho, "Capacity of MIMO wireless channel with full-duplex amplify-and-forward relay," in *Proc. of 2009 IEEE 20th International Symposium on Personal, Indoor and Mobile Radio Communications*, Tokyo, pp. 117-121, 2009. [Article \(CrossRef Link\)](#).
- [15] A. S. Arifin and T. Ohtsuki, "Ergodic capacity analysis of full-duplex amplify-forward MIMO relay channel using Tracy-Widom distribution," in *Proc. of Personal, Indoor, and Mobile Radio Communications (PIMRC), 2015 IEEE 26th Annual International Symposium on*, Hong Kong, pp. 266-270, 2015. [Article \(CrossRef Link\)](#).
- [16] H. Alves, D. Benevides da Costa, R. Demo Souza and M. Latva-aho, "On the performance of two-way half-duplex and one-way full-duplex relaying," in *Proc. of 2013 IEEE 14th Workshop on Signal Processing Advances in Wireless Communications (SPAWC)*, Darmstadt, pp. 56-60, 2013. [Article \(CrossRef Link\)](#).
- [17] H. Kim, S. Lim, H. Wang and D. Hong, "Optimal Power Allocation and Outage Analysis for Cognitive Full Duplex Relay Systems," *IEEE Transactions on Wireless Communications*, vol. 11, no. 10, pp. 3754-3765, October, 2012. [Article \(CrossRef Link\)](#).
- [18] L. Jiménez Rodríguez, N. H. Tran and T. Le-Ngoc, "Performance of Full-Duplex AF Relaying in the Presence of Residual Self-Interference," *IEEE Journal on Selected Areas in Communications*, vol. 32, no. 9, pp. 1752-1764, Sept. 2014. [Article \(CrossRef Link\)](#).
- [19] M. Feng, S. Mao, and T. Jiang, "Joint duplex mode selection, channel allocation, and power control for full-duplex cognitive femtocell networks," *Elsevier Digital Communications and Networks Journal*, vol.1, no.1, pp.30-44, Feb. 2015. [Article \(CrossRef Link\)](#).
- [20] M. Feng, S. Mao, and T. Jiang, "Duplex mode selection and channel allocation for full-duplex cognitive femtocell networks," in *Proc. of IEEE WCNC 2015, New Orleans, LA*, pp.1900-1905, Mar. 2015. [Article \(CrossRef Link\)](#).
- [21] N. Pappas, M. Kountouris, A. Ephremides and A. Traganitis, "Relay-Assisted Multiple Access With Full-Duplex Multi-Packet Reception," *IEEE Transactions on Wireless Communications*, vol. 14, no. 7, pp. 3544-3558, July 2015. [Article \(CrossRef Link\)](#).
- [22] A. D. Coso and C. Ibars, "Achievable rates for the AWGN channel with multiple parallel relays," *IEEE Transactions on Wireless Communications*, vol. 8, no. 5, pp. 2524-2534, May 2009. [Article \(CrossRef Link\)](#).
- [23] M. Zamani and A. K. Khandani, "Broadcast approaches to dual-hop parallel relay networks," in *Proc. of Information Theory Proceedings (ISIT), 2012 IEEE International Symposium on*, Cambridge, MA, pp. 1518-1522, 2012. [Article \(CrossRef Link\)](#).
- [24] O. Taghizadeh and R. Mathar, "Cooperative strategies for distributed full-duplex relay networks with limited dynamic range," in *Proc. of Wireless for Space and Extreme Environments (WiSEE), 2014 IEEE International Conference on*, Noordwijk, pp. 1-7, 2014. [Article \(CrossRef Link\)](#).
- [25] M. Yuksel and E. Erkip, "Diversity-Multiplexing Tradeoff in Cooperative Wireless Systems," in *Proc. of 2006 40th Annual Conference on Information Sciences and Systems*, Princeton, NJ, pp. 1062-1067, 2006. [Article \(CrossRef Link\)](#).
- [26] Y. Liu, X. G. Xia and H. Zhang, "Distributed Linear Convolutional Space-Time Coding for Two-Relay Full-Duplex Asynchronous Cooperative Networks," *IEEE Transactions on Wireless Communications*, vol. 12, no. 12, pp. 6406-6417, December 2013. [Article \(CrossRef Link\)](#).

- [27] M. Duarte, C. Dick and A. Sabharwal, "Experiment-Driven Characterization of Full-Duplex Wireless Systems," *IEEE Transactions on Wireless Communications*, vol. 11, no. 12, pp. 4296-4307, December 2012. [Article \(CrossRef Link\)](#).
- [28] Y. Ding, J. K. Zhang and K. M. Wong, "The Amplify-and-Forward Half-Duplex Cooperative System: Pairwise Error Probability and Precoder Design," *IEEE Transactions on Signal Processing*, vol. 55, no. 2, pp. 605-617, Feb. 2006. [Article \(CrossRef Link\)](#).
- [29] B. M. Hochwald and T. L. Marzetta, "Unitary space-time modulation for multiple-antenna communications in Rayleigh flat fading," *IEEE Transactions on Information Theory*, vol. 46, no. 2, pp. 543-564, Mar 2000. [Article \(CrossRef Link\)](#).
- [30] Y. Jing and B. Hassibi, "Distributed Space-Time Coding in Wireless Relay Networks," *IEEE Transactions on Wireless Communications*, vol. 5, no. 12, pp. 3524-3536, December 2006. [Article \(CrossRef Link\)](#).
- [31] R. B. Ash, "Lectures on Statistics," <http://www.math.uiuc.edu/~r-ash/Stat/StatLec21-25.pdf>
- [32] Y. Chang and Y. Hua, "Diversity analysis of orthogonal space-time modulation for distributed wireless relays," in *Proc. of Acoustics, Speech, and Signal Processing, 2004, Proceedings (ICASSP'04), IEEE International Conference on, IEEE*, vol. 4, pp. 561-564, 2014. [Article \(CrossRef Link\)](#).
- [33] A. Ghasemmehdi and E. Agrell, "Faster Recursions in Sphere Decoding," *IEEE Transactions on Information Theory*, vol. 57, no. 6, pp. 3530-3536, June 2011. [Article \(CrossRef Link\)](#).



Guoling Liu received his BS degree in communication engineering from College of Communication Engineering, Chongqing University in 2012. Currently he is studying for the Ph.D. degree in communication and information system at Chongqing University. His research focuses on full-duplex communication.



Wenjiang Feng received his Ph.D. degree in electrical engineering from Chongqing University in 2000. Currently, he is a professor at the College of Communication Engineering in Chongqing University. His research interests fall into the broad areas of communication theory, wireless communication.



Bowei Zhang received his BS degree in from College of Communication Engineering, Chongqing University, in June 2010. He is currently studying for his Ph.D. degree in communication and information system at College of Communication Engineering, CQU. His research interests include interference alignment, signal alignment and network coding in MIMO relay system.



Tengda Ying received the BS degree in communication engineering from Chongqing University, Chongqing, China, in 2013. He is currently working toward the Ph.D. degree with the Department of Communication and Information Systems where he studies the next generation wireless communication networks and involves a new interference management named Interference Alignment. His current research interests also include information theory and full-duplex communication.



Luran Lü received her BS degree in Chongqing University in June 2015. She is currently pursuing MS degree at College of Communication Engineering, Chongqing University. Her research fields include wireless network communication and full-duplex communication.